Chattering Suppression for DSP Based Sliding Mode Current Control of PM DC Drives

Dal, Mehmet; Teodorescu, Remus

Published in:
Proceedings of the 35th Annual Conference of the IEEE industrial Electronics Society

Publication date:
2009

Document Version
Publisher's PDF, also known as Version of record

Chattering Suppression for DSP Based Sliding Mode Current Control of PM DC Drives

Mehmet Dal [(1)] and Remus Teodorescu [(2)]
[(1)] Kocaeli University/ Electrical Department of VSK, Kocaeli, Turkey e-mail:mdal@kocaeli.edu.tr
[(2)]Aalborg University/Instituted of Energy Technology, Aalborg, Denmark e-mail: ret@iet.aau.dk

***Abstract*—This paper investigates several chattering suppression methods for DSP based implementation of sliding mode control (SMC). It concentrates on the 'equivalent-control-dependent' and 'state-dependent' gain adjustment methods proposed in recent theoretical studies, and tests the effectiveness of these proposals for current regulation of PM DC drives. The well-known observer-based method was also used for purposes of comparison. Additionally, increasing sampling rate was examined to determine how it affects the amplitude of discretization chattering. These methods may exhibit unsatisfactory results when performed separately, and so various combinations of these methods are tested to find the best solution for chattering elimination. Discontinuous control signal averaging, which is a common chattering reduction technique, is made possible while the system is online by the use of a tunable low-pass filter (LPF). Experimental results demonstrating the effectiveness of each method as well as a combined chattering elimination method are presented and discussed.**

***Index Terms*— DC drives, sliding mode control, chattering reduction.**

I. Introduction

In the last two decades, SMC has received more attention among control research communities due to its robustness and invariance to external disturbances and parametric uncertainties. Presently, SMC is widely accepted in nonlinear control areas to provide high performance in tracking control. However, to preserve the prospective benefits of SMC methodology, the phenomenon of so-called "chattering," which is the main obstacle encountered in real-time applications, has to be prevented.

Chattering is an undesired oscillation appearing on the system trajectory with finite frequency and amplitude. It is harmful because it leads to low control accuracy, high wear of moving mechanical parts, and high heat loss in power circuits; it may also degrade control loop stability [1], [2]. Two reasons for chattering have been identified [1]: 'unmodeled' dynamics of the system usually disregarded in the control design process, and the inherently limited sample rate in digital controllers. Several suppression methods concerning the first reason have been analyzed recently, including two gain adjustment methods and an observer-based method [3], [4]. The effectiveness of the gain adjustment methods has been verified by analysis and numerical simulation results for illustrative systems. However, their implementation in real-life systems has not been studied yet. The observer-based method is one of the most well-known ways to perform chattering suppression [1] [5], but parameter mismatches between the observer and the plant can degrade robustness [6]. Thus, the problem of robust control can be reduced to the problem of robust estimation.

On the other hand, SMC switching frequency depends on the sampling rate of the digital controller, which causes an undesired effect called discretization chatter. Hence, increasing the sampling rate may decrease the amplitude of the discretization chatter. The use of an LPF is common and fairly good at capturing the equivalent control from a discontinuous control signal in tracking control tasks [7]. However, the present study observed that neither the use of an LPF nor increasing sampling rate alone could remove chattering fully due to the presence of high gain in the controller. Chattering analysis devoted to second-order SMC and other reduction methods has been presented in [8], [9] and references therein.

This paper aims to find an efficient method for chattering suppression in real-time implementation of SMC. For this purpose a DSP-based DC drive system is considered to represent a real-life system, in which the hall-effect current sensor and transistorized H-bridge power converter together may exhibit similar behavior to an actuator that has second-order dynamics with a small time constant, and the rotor winding acts as a first-order system fed by a discontinuous switching control signal. This analogy may emphasize that the inner current control loop of the drive system has both chattering sources identified above, and it may be considered an adequate simple plant to investigate the chattering problem.

To determine the effectiveness of recent proposed chattering suppression methods- the 'equivalent-control-dependent' and 'state-dependent' gain adjustments are applied to current control of PM DC motor drives and compared to well-known observer-based method. To verify this idea a unified sliding mode observer is used for current estimation, and several experiments were conducted for the each method and various combined methods under various scenarios including the use of an increased sampling rate and the use of an adjustable LPF. The proposed methods and observer-based method are unsatisfactory when performed separately, and so various combinations of these methods are tested to find the best solution for chattering elimination. The results of these experiments are comparatively presented and discussed.

II. System Model and Sliding Mode Control

A. DC machine dynamic model

Permanent magnet DC machine dynamics can be expressed by the following two coupled first-order differential equations (the argument *t* is omitted for simplicity of notation):

$$L\frac{di}{dt} = -Ri + u - k_e\omega \quad (1)$$

$$J\frac{d\omega}{dt} = -B\omega + k_t i_a - t_L \quad (2)$$

Where u is the supply voltage, i is the rotor current, ω is the angular peed of the rotor shaft, t_L is the load torque, R and L are resistance and inductance of the rotor winding, respectively, k_e and k_t back-emf constant and torque constant of the motor, respectively, J is total motor and load inertia, and B is the viscous friction coefficient.

B. Sliding mode current controllers

The design of SMC involves two steps: (*i*) The selection of an appropriate switching function *s* for a desired sliding mode dynamics, and, (*ii*) the design of a control for enforcing a desired sliding motion on selected manifolds in system state spaces. In case of the current trajectory tracking, the required switching manifold can be described by

$$s = e_i = i^* - i \quad (3)$$

where e_i is the current tracking error, i is measured current and i^* it's reference normally obtained from output of outer loop controller, namely speed controller. Based on Lyapunov stability theorem to enforce a sliding mode on the selected sliding surface, the desired control must be satisfying existing condition $\dot{V} = s\dot{s} < 0$. This can be fulfilled with the following control

$$u_1 = -M\,sign(s) + u_{FF} \quad (4)$$

where $u_{FF} = k_e\omega$ is a feed-forward term corresponding to the back *emf* generated on the rotor winding, M denotes the control gain constant. In case of the function s is selected, evaluation of $s\dot{s}$ with help of (1) and (4) is resulted in

$$s\dot{s} = s\left(\frac{di^*}{dt} + \frac{R}{L}i\right) - \frac{1}{L}M|s| \quad (5)$$

which implies following condition for existing a sliding mode

$$|L\dot{i}^* + Ri| < M \quad (6)$$

Remark: An alternative choice for sliding function could be as $s_2 = c_i e_i + \dot{e}_i$. Accordingly, if sliding mode is enforced in a finite time interval then, asymptotic converge of the current error to zero is guarantied ($s_2=0$). But, s_2=0 as switching function can not be applied, since it depends on the time derivative of current which is discontinuous and the condition $s_2\dot{s}_2 < 0$ can not be fulfilled.

III. Chattering Suppression Methods

The chattering occurs mainly due to non-linear property of sign function which leads the switching operation, and generates a discontinuous control signal. The magnitude of chattering depends on switching control gain.

In this section, various chattering suppression methods proposed in [3], [4] briefly explained for current regulation of DC drives.

A. Averaging operation with LPF

In implementation of SMC, the use of a first-order LPF is a usual approximation to extract the equivalent control (Fig.1). When the implementation is performed by digital controllers, this can be assured by utilizing a discrete-time LPF which can be obtained by discretizing a first-order continuous-time LPF $\tau_c\dot{u}^* + u^* = u$ using Euler-method as follows.

$$\dot{u}^* = \frac{du^*}{dt} \cong \frac{u_k^* - u_{k-1}^*}{T_s}$$

$$u_k^* = \underbrace{\frac{T_c}{T_c + T_s}}_{a} u_{k-1}^* + \underbrace{\frac{T_s}{T_c + T_s}}_{1-a} u_k \quad (9)$$

where T_s is a sampling-time of digital controller, T_c is time-constant of LPF and u_k^* is average value of the control input u_k at k^{th} sampling interval. The block diagram Fig.1 obtained from (9) represents the structure of a discrete-time LPF with adjustable cut-off frequency. This structure enables corner frequency tuning on-line, and facilitates extraction of the equivalent control practically. This structure can be used for the rotor angular speed estimation too. The filtering also attenuates the chattering by averaging the discontinuous control signal.

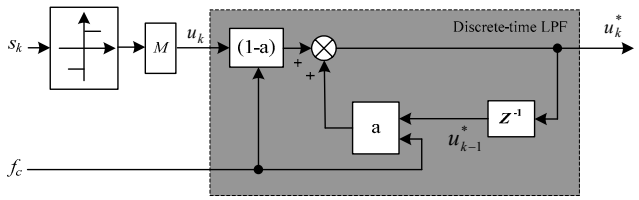

Fig.1. Averaging discontinuous control signal and the structure of a tunable discrete-time first-order LPF with adjustable cut-off frequency

B. State-observer-based method

The main purpose for using an observer is to exclude unmodeled dynamics from the main control loop [6]. As shown in Fig.2, the sliding manifold is constructed by using estimated current $\hat{i}$ instead of measured current i. Therefore, the auxiliary observer loop can be left free of any unmodeled dynamics caused by the combined use of a current sensor and a power-converter. In order to estimate rotor current, the unified sliding mode observer (10) proposed in [1] is used.

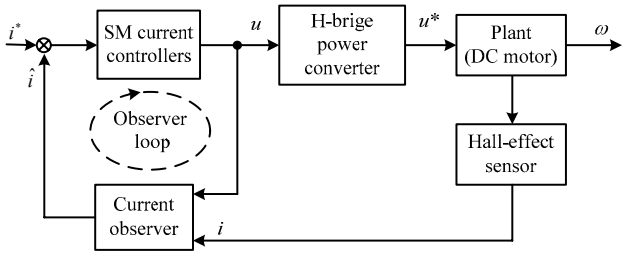

Fig.2. Observer-based sliding mode current control of DC drive system

$$\frac{d\hat{i}}{dt} = -\frac{R}{L}\hat{i} + \frac{1}{L}u - l_1 sign(\hat{e}_i) \tag{10}$$

where $\hat{e}_i (= \hat{i} - i)$ denotes currents estimation error, and $l_1 > 0$ is a constant gain. From (1), (10) the estimated current error dynamics can be yielded as

$$\frac{d\hat{e}_i}{dt} = -\frac{R}{L}\hat{e}_i + \frac{k_e}{L}\omega - l_1 sign(\hat{e}_i) \tag{11}$$

According to the existing condition $s\dot{s} < 0$, if the gain l_1 is selected as follows then a sliding mode $(s = \hat{e}_i = 0)$ occurs.

$$|(k_e / L)\omega| < l_1 \tag{12}$$

For a proper current estimation with the observer (10) the average value of term $l_1 sign(\hat{e}_i)$ is required. The average value $(l_1 sign(\hat{e}_i))_{eq}$ is the equivalent control which can be obtained passing term $l_1 sign(\hat{e}_i)$ through an LPF. Then the estimated rotor shaft angular speed $\hat{\omega} = (l_1 sign(\hat{e}_i))_{eq} / k_e$ can be obtained and may be used for purpose of speed sensorless drives.

Another option to estimate the current is well-known Luenberger observer:

$$\frac{d\hat{i}}{dt} = -\frac{R}{L}\hat{i} + \frac{1}{L}u - \frac{k_e}{L}\omega + l_2(\hat{i} - i) \tag{13}$$

which can also be realized to construct a sliding manifold for the chattering reduction purpose. Determining the value of gain l_1 plays vital role to get a satisfied convergence of the current estimate for both observers (10) and (13). The construction of the observer (10) with Simulink blocks is shown in Fig.3.

C. State-dependent gain method

In [4], based on describing function analysis it is proven that amplitude of the chattering proportionally depends on the switching control gain M. Therefore any methods would be helpful to suppress chattering if it can decrease the gain M properly without lose the existence of sliding mode. In this method value of the gain M is reduced along system state

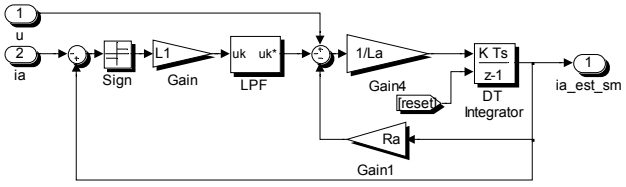

Fig.3. Structure of realized sliding mode current observer

without scarifying converge rate of trajectory tracking. For implementation of the state dependent gain method, the sliding function is selected as in (3) and the current control law with a feed-forward term u_{FF} can be described, respectively, as follows:

$$\begin{aligned} s_i &= e_i (= i^* - i) \\ u_2 &= \underbrace{-M(|e_i| + d_1)}_{M(e_i)} sign(s_i) + u_{FF} \end{aligned} \tag{14}$$

where d_1 is a sufficiently small constant. This structure has the sate depended control gain $M(e_i)$ and may replaced with (4) to attenuate chattering. The control inputs in general are bounded for all physical systems, therefore (14) may be modified by adding a limiter, which converts the system into 'the variable structure'.

$$u_2^* = \begin{cases} u_{\max} & if \quad u \ge u_{\max} \\ -M(|s_i| + d_1) sign(s_i) + k_e\omega & if \quad |u| < u_{\max} \\ -u_{\max} & if \quad u \le u_{\max} \end{cases} \tag{15}$$

In our case, the control input is bounded by DC link voltage Vdc(=$u_{\max}$).

D. Equivalent-control-dependent gain method

The state tracking error dynamics for the current control of DC drives can be given in general form of

$$\frac{de_i}{dt} = f(i,t) - \frac{1}{L}u \tag{16}$$

where $f(i,t) = i^* + (R/L)i + (k_e/L)\omega$, then a possible control law may be

$$\begin{aligned} s_i &= e_i (= i^* - i) \\ u_3 &= M(|\eta| + d_2) sign(s_i) + u_{FF} \end{aligned} \tag{17}$$

where M and d_2 are positive constants, η is average value of $sign(s_i)$, which is equals to estimated equivalent control $\hat{u}_{eq}$. The average value of $sign(s_i)$ can be acquired by using a LPF $\tau\dot{\eta} + \eta = sign(s_i)$. The time constant for the LPF should be selected as $\tau << 1$. If the control input inserted into (15) derivative of sliding function (s_1) is resulted in

$$\frac{ds_i}{dt} = f(i,t) - \frac{1}{L}M(|\eta| + d_2)sign(s_i) + \frac{1}{L}k_e\omega$$
$$= L\dot{i}^* + Ri - M(|\eta| + d_2)sign(s_i) \quad (18)$$

where $\dot{i}^* (= di^*/dt)$ denotes the derivative of the reference current. This finding implies that, the existence of sliding mode depends on holding the following condition

$$|Li^* + Ri| < M\ |\eta| \quad (19)$$

IV. Hardware Set-up and Experiments

Experimental implementations were conducted using a hardware setup called the 'DC Experimental System', which includes a small-sized permanent magnet ESCAP DC motor driven though an H-bridge converter by a DSP-2 controller board. A useful guide for the DSP-2 experimental system can be found in [10]. The DSP-2 controller board can communicate with a PC through to a serial RS-232 cable or USB port, and is based on the TI TMS320C32-60 core and the FPGA Xilinx CS40-PQ240. The additional toolbox software 'DSP-2 Library' runs under Matlab/Simulink, eliminates the need for hand code generation, and offers its own rapid control prototype. The 'DSP-2 Terminal' software enables data visualization and parameter tuning during the operation interval, and is run on the host PC. The nominal parameters and rated data of the driven motor are listed in Table1.

A block diagram depicting the overall structure of the drive system is given in Fig.4. The control algorithm is programmed with Matlab/Simulink blocks, which can be directly built in, and executed with a sample time of 200μsec via the DSP-2 controller. As shown in Fig.4, a flywheel is mounted on the rotor shaft to cause the motor to receive a considerable amount of load current. The switch s_1 is used to enable system operation with or without a speed controller, and s_2 is used to select a current feedback signal (estimated or measured current). When the speed controller is excluded from the loop by switch s_1, the motor can be driven by the current controller alone, which applies a command given by the current reference generator. In this case, a square-wave current reference is provided to facilitate the repeated capturing of the current

TABLE I
Name Plates And Nominal Parameters of The Motor

Quantity	Symbols	Unites
Nominal voltage	V_{dc}	12 V
No-load speed	n	5800rpm
Max. continuous current	I_a	1.5A
Max. continuous torque	$T_{e\text{-}max}$	28.4 mNm
Back-EMF constant	K_e	0.0195 V.s/rad
Torque constant	K_t	0.0195 N.m/A
Rotor resistance	R	2.5 Ω
Rotor inductance	L	0.3 mH
Inertia of Motor	J	17.2e-7 kg.m2
Viscous damping constant	B	1e-6 N.m.s/rad

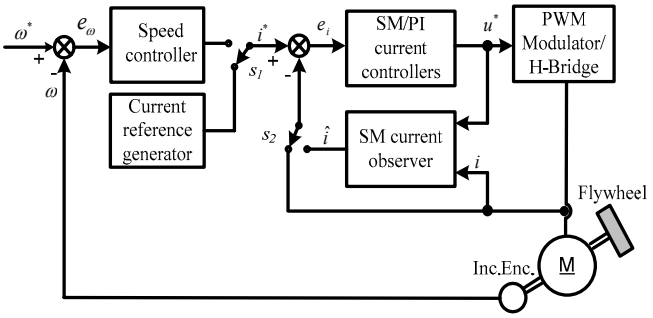

Fig.4. Structure of DC motor drive system used in experiments

transient response. Three different versions of control laws, u_1, u_2, u_3 in (4), (14) and (17), respectively, were performed in turn to regulate the rotor current. All control scheme structures are shown together in Fig.5.

The following tests were performed:

Test1: a) To exclude the effects of the observer method, the measured current i was used instead of the estimated current $\hat{i}$ in the current feedback loop, and then to expose how the each control law alone reduces chattering, the control laws u_1, u_2 and u_3 were each executed in turn using the same sampling time of 200μsec. b) To examine how the observer method alone attenuates chattering, the auxiliary observer loop was activated by switch s_2, replacing the measured current i with estimated current $\hat{i}$ and the test was repeated (results are presented comparatively in Fig.6). We remind that the control laws u_2 and u_3 have a gain adjustment mechanism, and even though the same gain constant value M=12 was used for all of the control versions, the magnitude of the discontinuous control signal generated by the second and third control versions obtained was lower than that of the first one. This can be seen by comparing the responses in (b) and (c) with (a) in Fig.6. These results verify that reducing the value of gain constant M attenuates the chattering magnitude, and that the gain adjustment mechanisms employed in (15) and (17) perform efficiently.

Test2: To expose how the increase in the sampling rate reduces discretization chatter, Test1 was repeated using a shorter sampling time of 100μsec. The resulting data is presented in Fig.7, which verifies that increasing sampling rate attenuates chattering especially well for the control version u_2.

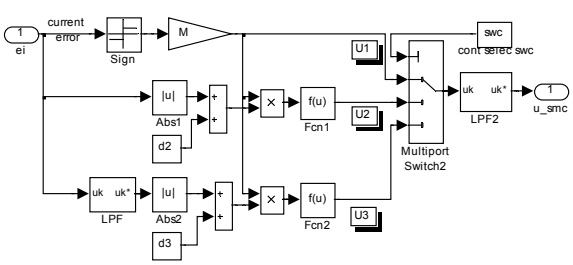

Fig.5. Structure of the current controllers u_1, u_2 and u_3 all together

Test3: The observer-based method was examined for control laws u_1, u_2 and u_3 using the same sampling time of 100μsec. The data recorded in this test is plotted in Fig.8, which verifies that the observer-based method reduces chattering considerably, and has virtually the same effects as all other control versions.

Test4: With the speed control loop closed (via s_1), the control laws u_1 and u_2 were examined with and without the observer method. In these cases, the current reference signal is provided by the speed controller, and a current limiter is required to ensure that the system operates in current control mode when armature current exceeds its rated value during transient periods or overloading. The Test4 data is plotted in Fig.10-11, which demonstrates that the proposed current control laws remain valid even when the speed control loop is closed.

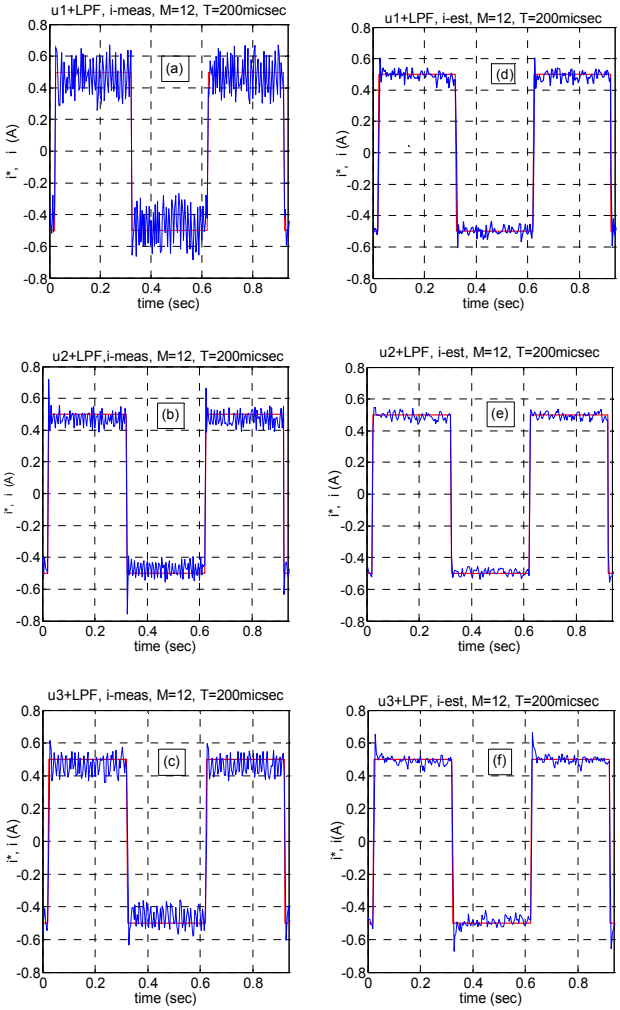

Fig.6. The recorded results of Test1 (in the first column) and Test2 (in the second column). In both columns, the traces show the current trajectory response provided by control laws u_1, u_2 and u_3, respectively.

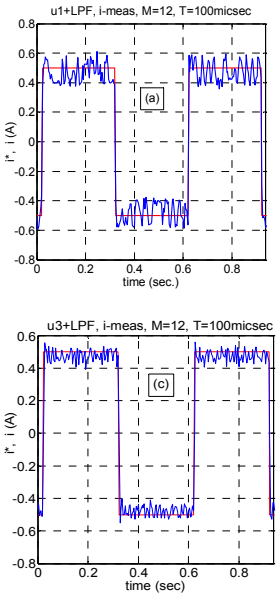

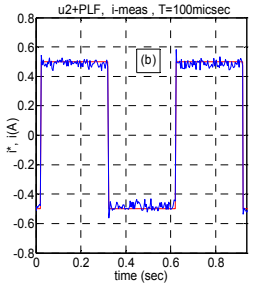

Fig.7. The recorded results of Test2, when an increased sampling time of 100μsec were used and observer was missed. The traces in (a), (b), (c) are current trajectory responses obtained for the control laws u_1, u_2 and u_3 respectively.

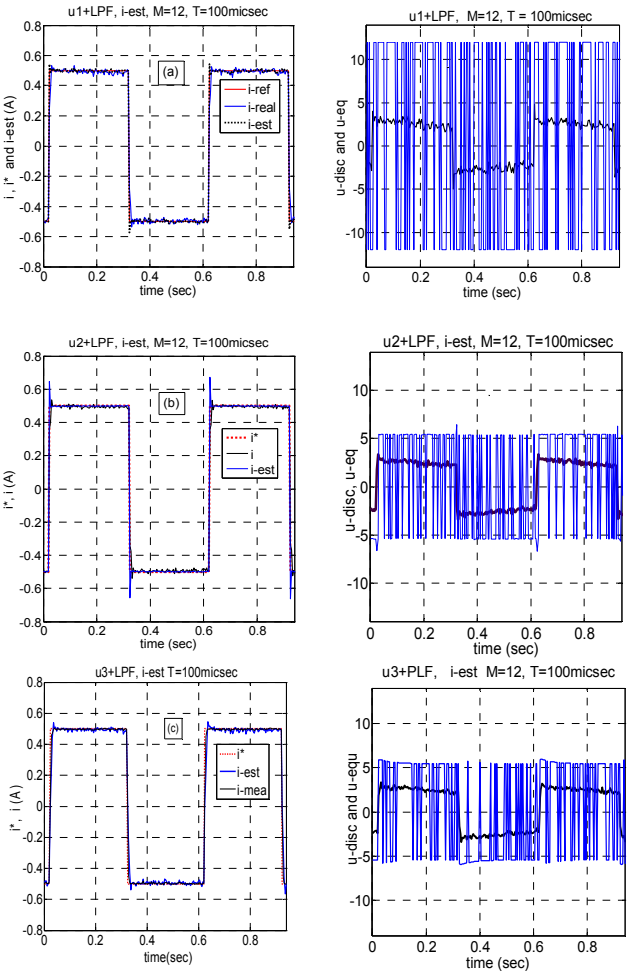

Fig.8. The recorded results of Test3. In the first column, the traces show currents i^*, $\hat{i}$ and i together for the controls u_1, u_2 and u_3, respectively. The second column shows the corresponding discontinuous control input and its average value when the observer-based method was used with an increased sampling rate.

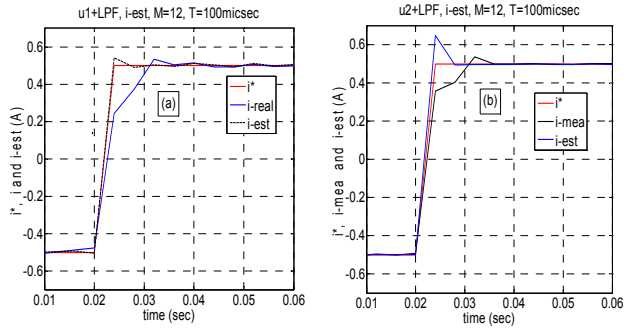

Fig.9. Enlargement of Fig.8 (a) and (b), the convergence of current estimate.

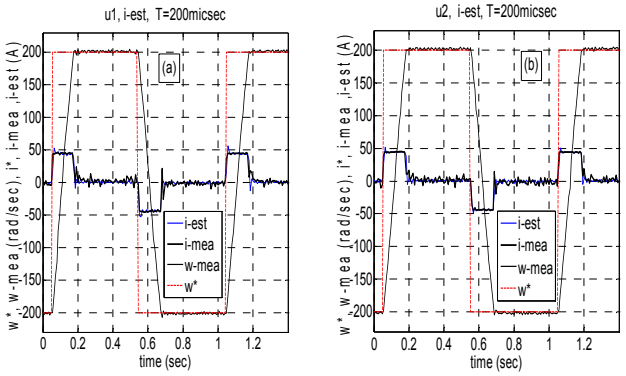

Fig.10. The recorded results of the Test4, the rotor current and speed response to a square-wave speed trajectory for control law u_1 (a) and control law u_2 (b). In the both figures the traces with high amplitude show the reference and measured speeds, and those with low amplitude show the measured and estimated currents (multiplied by 30).

Moreover, a conventional proportional plus integral (PI) current controller was examined for the purpose of performance comparison with SM current controllers, as well as to determine how the current tracking performance can be improved when the estimated current is used in feedback loop

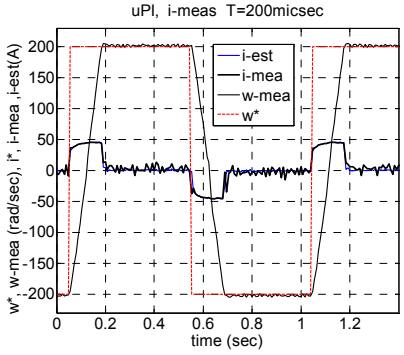

Fig.11. The rotor current and speed response to a square-wave speed trajectory for the PI current controller with the measured current feedback, the traces with the high amplitude show the reference and measured speed, and with the low amplitude show the measured and estimated currents (multiplied by 30).

instead of the measured current for PI controller. The recorded data in the latter test is plotted in Fig.11, which verifies that the mixed SM current controller provides faster current tracking performance as well as a current ripple level similar to the PI current controller.

V. Conclusion

In this paper, several chattering suppression methods for current regulation of DC motor drives were examined in real-time. It was experienced that chattering elimination is not a trivial problem for digital implantation of SMC, and that discretization chatter may be indistinguishable from chattering caused by unmodeled system dynamics.

The gain adjustment and state-observer-based methods attenuate chattering considerably but do not eliminate it fully. However, experimental results demonstrated that the best way to suppress chattering may be a mixed method which combines the state-observer and gain adjustment methods while using an increased sample rate and an LPF. This may increase the complexity of the control structure but offers the advantages of SMC methodology– robustness and fast dynamic response. Moreover, a performance comparison between the SMC-based scheme and conventional PI demonstrated that the mixed SMC scheme exhibits a faster transient response than a conventional PI current controller while maintaining a similar current ripple level.

References

[1] V. I. Utkin, J. Gulder, and J. Shi, "Sliding Mode Control in Electromechanical Systems," London, U.K.: Taylor & Francis, 1999.

[2] H.K. Halil, "Nonlinear System," New Jersey: Pearson Educ. Inc., 2000.

[3] V. I. Utkin, H. Lee "The chattering problem in sliding mode system" *Proce. of the International Workshop on Variable Structure Systems* Alghero, Italy, June 5-7, 2006

[4] V. I. Utkin, H. Lee "The chattering analysis" *Proc. of 12th International Power Electronics and Motion Control Conference on Ind.* EPE_PEMC, Portoroz, Slovenia 2006.

[5] A. G. Bondarev, S. A. Bondarev, N. E. Kostyleva, and V. I. Utkin,"Sliding modes in systems with asymptotic state observers," *Autom.Remote Control*, vol. 46, no. 6, pp. 679–684, 1985.

[6] K. D. Young, V. I. Utkin, and U. Ozguner, "A control engineer's guide to sliding mode control," *IEEE Trans. Control Syst. Technol.*, vol. 7, no. 3, pp. 328–342, May 1999.

[7] J.X. Xu, Y.J. Pan and T. H. Lee, "Sliding Mode Control With Closed-Loop Filtering Architecture for a Class of Nonlinear Systems ," *IEEE Trans. Circuits and Sys.*: Express Briefs, vol. 51, No. 4, pp. 168-173, Apr. 2004.

[8] I. Boiko, L. Fridman, A. Pisano and E. Usai "Analysis of Chattering in Systems with Second-Order Sliding Modes" *IEEE Trans. Autom. Control*, vol. 52, no. 11, pp. 2085–2101, Nov. 2007.

[9] G. Bartolini, A. Ferrara, and E. Usai, "Chattering avoidance by second order sliding mode control," *IEEE Trans. Autom. Control*, vol. 43, no. 2, pp. 241–246, 1998.

[10] User manual for programming DSP-2, "DC experimental system", Maribor University , Slovenia, 2004.